*34th EPS Conference on Plasma Phys. Warsaw, 2 - 6 July 2007 ECA Vol.**31F**, P-4.106 (2007)*

Evaluations of CXRS signals in fusion plasmas for various impurity species, spectral ranges and beam energies

V.Yu. Sergeev[1], R. K. Janev[2], A. V. Maksimov[1], I. V. Miroshnikov[1], C. L. Liu[3], N. Tamura[4], S.Sudo[4]

[1] *State Polytechnical University, St.Petersburg, Russia*
[2] *Macedonian Academy of Sciences and Arts, Skopje, Macedonia*
[3] *Institute of Applied Physics and Computational Mathematics, Beijing, P.R. China*
[4] *National Institute for Fusion Science, Gifu, Japan*

Introduction. Observation of Charge eXchange Recombination Spectroscopy (CXRS) signals is the basis of many plasma diagnostic applications. One of the examples is the TESPEL diagnostics studies of impurity transport in fusion devices [1]. Optimization of the CXRS signal with respect to the impurity tracer material, spectral range and plasma conditions is a prerequisite for the success of this diagnostic tool. In Ref. [2] a model for such an optimization of CXRS TESPEL diagnostics in LHD was developed. The model solves the collisional-radiative model equations for the populations of '*n,l'*-states of a hydrogen-like impurity under coronal equilibrium (CE) ionization conditions. The model was applied to the LHD TESPEL diagnostics in the visible range, with a hydrogen neutral beam energy E_{NBI} = 150 keV. For the fixed spectral range and beam energy conditions, the optimization of the CXRS signal was performed with respect to the selection of tracer impurity species. In the present work we generalize this model to optimize the CXR signal with respect to the beam energy, impurity material and the spectral range simultaneously.

Further model development. The basic assumptions of the Ref. [2] optimization model are kept unchanged. The essential simplification is made by taking into account the fact that the decay probability of an *nl*-state *via* transitions within the same principal quantum number *n* is much larger than *via* transitions with different *n* (see [3]). This, coupled with the strong collisional *l*-mixing, leads to a fast redistribution of direct CX population over *l* levels within a given *n*. Therefore, in calculating the radiative cascade matrix, one can use the statistical *l* distribution, $(2l+1)/n^2$, and partial charge exchange cross-section $\sigma_{CX}(n)$ instead of $\sigma_{CX}(n,l)$.

The $\sigma_{CX}(n)$ cross sections have been calculated by using the classical trajectory Monte Carlo (CTMC) method for E = 25, 50, 75, 100, 150 and 250 keV beam energies and fully stripped impurities with Z = 3, 6, 9, 12, 18, 22, 26, 30. By using appropriately scaled *n* and *E*, it was possible to represent all this large set of cross section data by a single, scaled cross section, $\sigma_{CX,sc}(n,Z,E)$, with an accuracy of 10%. The obtained *n*- and *Z*- scaled form of the

partial cross section $\sigma_{CX}(n,Z,E)$ allows one to optimize the CXR signal for any spectral range, with respect to parameters Z and E, and thereby generalizes the optimization model developed in Ref.[2].

The use of statistical distribution of l-substates within a given n, significantly simplifies the calculation of capture-radiation cross-section (see Eq. (8) in Ref. [2]), which now takes the form

$$\left\langle \sigma^{CX}_{n,(n-1)} \right\rangle = \sum_{l=0}^{n-1} (\sigma^{CX}_{n} + \sum_{n'>n} C_{n',n}\sigma^{CX}_{n'}) \times (2l+1)/n^2 \times P_{nl,(n-1)l'} , \qquad (1)$$

where $C_{n',n}$ is the cascade matrix from all levels $n' > n$ calculated in Ref. [4] and $P_{nl,(n-1)l'}$ is the radiation probability calculated in Ref. [3].

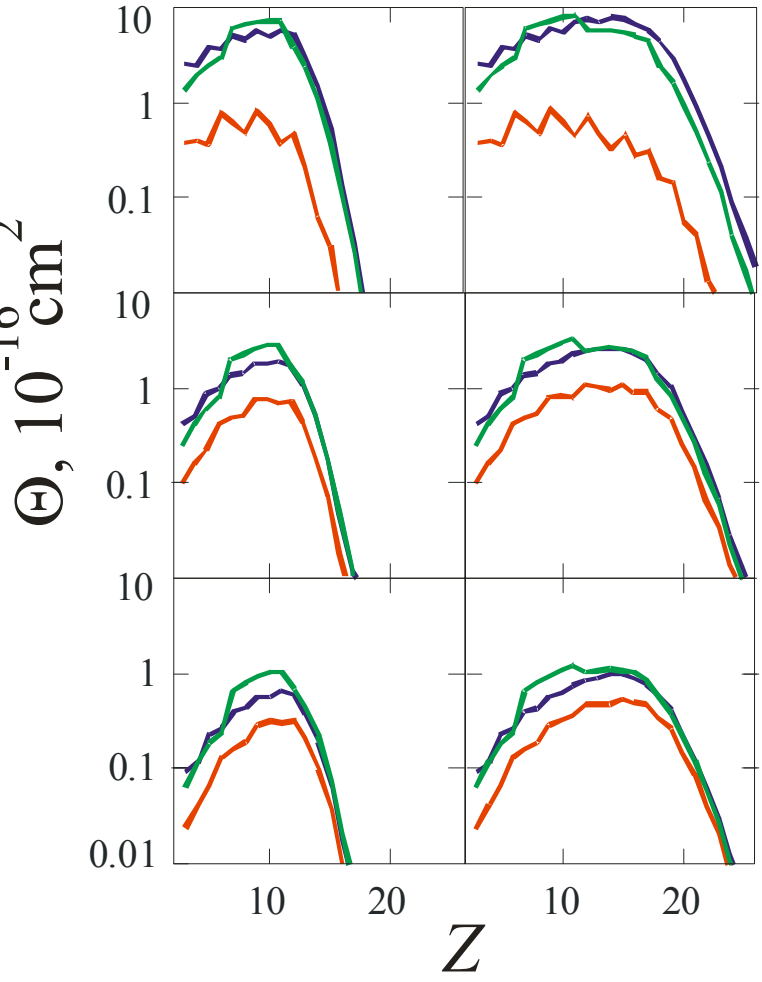

Fig. 1. *Θ(Z) dependencies for E = 50 keV (upper row), 100 keV (middle row), 150 keV (bottom row), for EUV (green curves), VUV (blue curves) and VISible (red curves) spectral ranges and for T_e = 1 keV (left column) and 3 keV (right column).*

It has been shown in Ref. [2] that at a fixed geometry of the experiment, NBI energy and power, the CXR signal is proportional to both $\left\langle \sigma^{CX}_{n,(n-1)} \right\rangle$ and the density of injected impurity nuclei in the charge state Z, N^Z. For a given plasma temperature T_e, N^Z and the total density of injected impurity, N_{imp}, are related by: $N^Z = \alpha_Z(T_e)\, N_{imp}$, where $\alpha_Z(T_e)$ is the ionization degree). Hence, the CXR signal is proportional to the product $\Theta(Z) = \left\langle \sigma^{CX}_{n,(n-1)} \right\rangle \times \alpha_Z$.

Results and discussion. The $\Theta(Z)$ dependences were calculated for neutral beam energies E = 50, 100, 150

keV, for the EUV (10 nm), VUV (100 nm) and VISible (420 nm) spectral ranges and for electron temperature T_e = 1 keV and 3 keV. These values of E, T_e and denotations of spectral ranges are arguments of Θ correspondingly. They are shown in Fig. 1.

The non-monotonic behavior of Z-dependencies, reflecting the discreteness of n- energy levels, is more pronounced for the lower wave lengths and smaller beam energies. Fig. 1 shows that the CXR signal generally increases with increasing the electron temperature and decreases with increasing the beam energy. Although measurements in the visible spectral range are from technical point of view the easiest ones, they have no essential improvement of the CXR signal by decreasing the beam energy. The EUV and VUV CXR signals demonstrate similar behavior and signal levels which up to one order of magnitude can be bigger than the ones for the visible spectral range (upper right plot in Fig. 1).

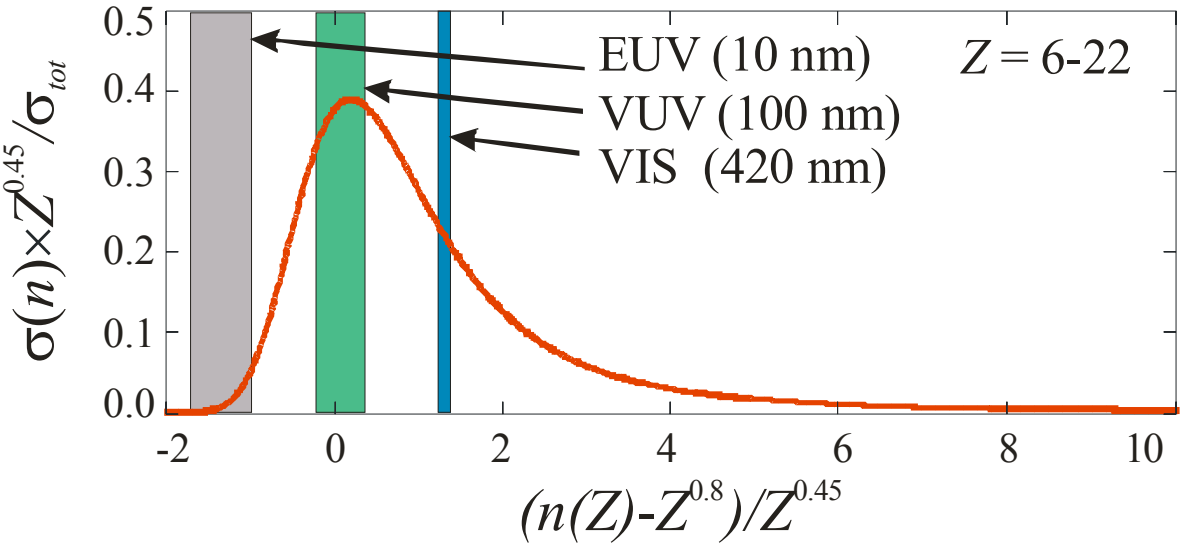

Fig. 2. *Reduced CX cross-sections versus reduced Z for E = 100 keV beam energy.*

The tendencies in the behavior of $\Theta(Z)$ observed in Fig.1 can be understood taking into account the role of cascade processes in the CXR signal. In Fig. 2 we show the reduced CX cross-sections versus the reduced Z for E = 100 keV. The hatched areas indicate the values of the (reduced) CX cross section (for this energy) for population of the level radiating in the EUV, VUV, VIS range, when the impurity charge varies between Z=6 (upper edge of the area) and Z = 22 (lower edge). One can see from this figure that in the case of the visible range the cross section for electron capture to the radiating level is well beyond the cross section maximum, for the VUV range it is around the cross section maximum, and for the EUV range it is again far from the cross section maximum. However, since for the

considered beam energy (100 keV), the *n*- distribution of captured electrons is rather broad, the cascading from the levels above the radiating one may give a significant contribution to its population. Fig. 2 shows that in the case of the visible range the cascade contribution is not very large, but in the case of VUV, and especially in the case of EUV spectral range, this contribution is substantial. As already obvious from Eq. (1), the value of capture-radiation cross section depends on both the cross section for direct electron capture to the radiating level and on the cascade contribution from the upper levels.

One should note that VUV technique is more suitable for studies of CXR signals of different impurity materials because in the EUV range a change of studied wave length is more complex and requires changing the number of multiple (and expensive) mirrors.

The maximum CXR signals in the VUV spectral range and E =50 keV are for Z = 6-16.

Conclusions. The calculated CXR signals generally increase with increasing the electron temperature (i.e. increase of $\alpha_Z(T_e)$) and with the decrease of beam energy (increase of σ_{CX}). Although measurements in the visible spectral range are easiest from technical point of view, they do not provide essential increase of the CXR signal by decreasing the beam energy. The EUV and VUV CXR signals exhibit similar general behavior, but their levels can be up to an order of magnitude larger than those in the visible spectral range. Taking into account the technical aspects, the VUV technique appears to be more suitable for studies of CXR signals of different impurity materials than the EUV technique.

References

[1] Sudo S., Plasma Fusion 69 (1993) 1349.

[2] V.Yu. Sergeev, R.K.Janev, M.J.Rakovic, *et al*., Plasma Phys. Contr. Fus. 44 (2002) 277.

[3] Bethe H A and Salpeter E E 1957 *Quantum mechanics of one- and two-electron atoms* Springer-Verlag, Berlin –Goettingen- Heidelberg, p. 262.

[4] Sobelman I I, Vainshtein L A, Yukov E A 1981 *Excitation of Atoms and Broadening of Spectral Lines* Springer-Verlag, Berlin –Heidelberg- New York.